CHEMISTRY
A EUROPEAN JOURNAL

FULL PAPER

DOI: 10.1002/chem.201200705

# Herringbone and Helical Self-Assembly of π-Conjugated Molecules in the Solid State through CH/π Hydrogen Bonds

**Mahima Goel and Manickam Jayakannan*[a]**

**Abstract:** Self-organization of organic molecules through weak noncovalent forces such as CH/π interactions and creation of large hierarchical supramolecular structures in the solid state are at the very early stage of research. The present study reports direct evidence for CH/π interaction driven hierarchical self-assembly in π-conjugated molecules based on custom-designed oligophenylenevinylenes (OPVs) whose structures differ only in the number of carbon atoms in the tails. Single-crystal X-ray structures were resolved for these OPV synthons and the existence of long-range multiple-arm CH/π interactions was revealed in the crystal lattices. Alignment of these π-conjugated OPVs in the solid state was found to be crucial in producing either right-handed herringbone packing in the crystal or left-handed helices in the liquid-crystalline mesophase. Pitch- and roll-angle displacements of OPV chromophores were determined to trace the effect of the molecular inclination on the ordering of hierarchical structures. Furthermore, circular dichroism studies on the OPVs were carried out in the aligned helical structures to prove the existence of molecular self-assembly. Thus, the present strategy opens up new approaches in supramolecular chemistry based on weak CH/π hydrogen bonding, more specifically in π-conjugated materials.

**Keywords:** helical structures · hydrogen bonds · liquid crystals · self-assembly · supramolecular chemistry

## Introduction

Solid-state self-assembly of π-conjugated organic molecules into hierarchical architectures and mapping out the origin of their secondary interactions are emerging as challenging tasks in the area of supramolecular chemistry.[1,2] The optical and electronic features of devices made up of these π-conjugated materials could directly be correlated to the precise arrangements of molecules in the solid state.[3,4] Though a sizeable amount of research has already been done on solvent-assisted self-assemblies of π-conjugated materials in solution,[5–7] their packing in the solid state is understood only at a premature level. This is partially associated with the scarcity of single-crystal structures for large π-conjugated synthons which produce higher order supramolecular assemblies in the solid state. Recently, a few efforts have been made to resolve the single-crystal structures of thin-film transistor materials such as pentacene and thiophene derivatives.[8] Contrary to expectations, it was found that these molecules arrange with edge-to-face orientation in herringbone motifs rather than face-to-face π stacks.[9] Most of the π-conjugated oligomers did not form single-crystal structures, and those which produce good crystals were found to be lacking macroscopic self-organization such as liquid crystallinity in the solid state.[10] Furthermore, packing of the chromophores in the crystal lattices was found to be highly sensitive to the structure of the π-conjugated backbone; as a result, diverse self-organization in an identical π-conjugated backbone was found to be very rare.[11] Herringbone motifs were restricted only to planar π-conjugated molecules whose structures were devoid of any substituent at the central aromatic core.[12] Unfortunately, such structural restrictions in the π-conjugated systems result in poor solubility and nonprocessability. As a consequence, solid-state ordering of the π-conjugated molecules beyond the herringbone motif was not studied. Unlike synthetic molecules, biomacromolecules like proteins have been shown to cleverly make use of weak noncovalent forces such as CH/π hydrogen-bond interactions to produce well-defined secondary or tertiary structures.[13] The CH/π interactions have been projected as one of the main driving force in the complex formation of proteins with cofactors and stabilization of water molecules in the hydrophobic cavity, for example, for photosynthesis.[14] The CH/π interactions were also observed in chemical research[15] in organic molecules and inorganic crystals;[16] however, their full potential has not been exploited to obtain any types of hierarchical supramolecular assemblies.[11a] π-Conjugated oligomers (or polymers) are one of the most promising chemical motifs for studying CH/π interactions in the self-assembly approach because they have 1) rigid aromatic π-conjugated backbones (or extended π systems) which can serve as H-bond acceptors and 2) flexible alkyl chains anchored on the periphery for solubility purposes, which can behave as H-bond donors (CH groups).

[a] M. Goel, Dr. M. Jayakannan
Department of Chemistry
Indian Institute of Science Education and Research
Dr. Homi Bhabha Road, Pune 411008, Maharashtra (India)
Fax: (+91) 20-2590 8186
E-mail: jayakannan@iiserpune.ac.in

Supporting information for this article is available on the WWW under http://dx.doi.org/10.1002/chem.201200705.

Recently we showed that the viability of CH/π interactions in π-conjugated species is highly dependent on appropriate design of the chromophore structure in hydrocarbon- and fluorocarbon-tailed oligophenylenevinylenes (OPVs).[17]

The present approach demonstrates the potential of CH/π interaction in making hierarchical supramolecular structures like three-dimensional helical assemblies and herringbone motifs of π conjugates in the solid state. The structures of the OPV synthons were very carefully chosen with three important components: 1) a distyrylbenzene core as π acceptor, 2) tricyclodecanemethylene (TCD) bulky units in the middle as CH donors, and 3) alkyl tails of different lengths as self-assembly directors (see Figure 1). The OPVs reported


Figure 1. Diverse self-organization of OPVs in the solid state.

here are so simple as their structures differ only in the number of carbon atoms in the alkyl tails. The uniqueness of the TCD-OPV design is that it is devoid of strong intermolecular interactions and only can self-organize via weak noncovalent forces such as aromatic π stacking, CH/π interactions, and van der Waals interactions, the energy terms of which are less than 1–4 kcal mol$^{-1}$. Single-crystal structures of OPV molecules were resolved to establish the role of CH/π interactions and the origin of self-assembly at the molecular level. Further, crystallographic parameters such as pitch and roll angles and their displacements were determined to establish the correlation between crystal structures and liquid-crystalline (LC) mesophase morphology. The findings revealed that the self-organization of π-conjugated species underwent transformation from 2D herringbone layer to 3D helical twist in the liquid crystalline mesophases. Circular dichroism studies on the OPVs revealed that the helical structures were produced only on aligning the chromophores in the LC mesophase, and they were completely lost in solution. Thus, the CH/π interaction has been proven to be an important noncovalent force in the molecular self-assembly of organic solids, more specifically in π-conjugated organic molecules.

## Results and Discussion

Synthetic details, structural characterization, thermal analysis, and polarizing microscopy studies are provided in the Supporting Information. The TCD-OPVs with short tails ($n$ = 0–4 C atoms) were found to be crystalline solids, whereas increasing the tail length ($n$ = 5–9) resulted in thermotropic cholesteric liquid crystals.[18] The long-tailed OPVs ($n$ = 10-15) produced hierarchical helical, ring-banded supramolecular assemblies (see Figure 1). In the absence of crystallographic evidence, based on photophysical characterization and other analysis, the mechanism for this diverse self-organization in TCD-OPVs was proposed on the basis of aromatic π stacking and van der Waals interactions.[18a] Herein, single-crystal structures of OPVs belonging to each category of mesophases were successfully obtained: OPV-4 (crystalline solid), OPV-8 (short-pitch cholesteric), and OPV-12 (helical bands) to trace the noncovalent interactions behind these diverse LC mesophase organization in the solid state. The crystal structures of the OPVs are shown in Figure 2, and their unit-cell parameters are provided in the Supporting Information (SF1 to SF-3 and ST1). All three

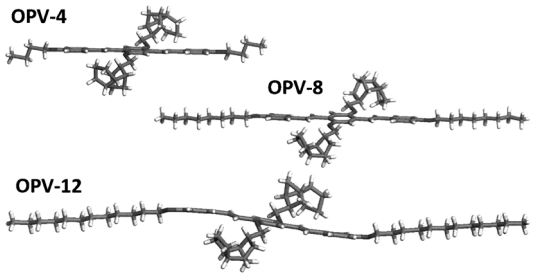


Figure 2. Single-crystal structures of OPV-4, OPV-8, and OPV-12.

benzene rings in the OPVs are in the same plane and constituted the molecular axis. OPV-4 has symmetric structure and crystallizes in monoclinic space group $P2_1/n$, whereas OPV-8 and OPV-12 crystallize in noncentrosymmetric triclinic space groups. The TCD units attached at the center occupy either side of the plane perpendicular to the aromatic backbone. The two alkyl tails on the terminal aryl rings are on the same plane constituted by the aromatic rings. The crystal of OPV-8 contains one solvent molecule per structure, but the solvent molecules are not involved in any type of secondary interactions. The butyloxy tail in OPV-4 has one *cis* conformation, whereas the octyl and dodecyl tails are aligned in all-*trans* conformations in OPV-8 and OPV-12. The torsion angles from the central aromatic ring to either side are 9.93 and 6.29° in OPV-12, 10.95 and 11.94° in OPV-8, and symmetric 6.88° in OPV-4. These values indicate that the OPV backbone is indeed planar in all three

  

cases, but they differ in the orientation of alkyl tails along the molecular axis.

The three-dimensional packing of all three OPVs is shown in Figure 3. The bulky TCD units protrude from the

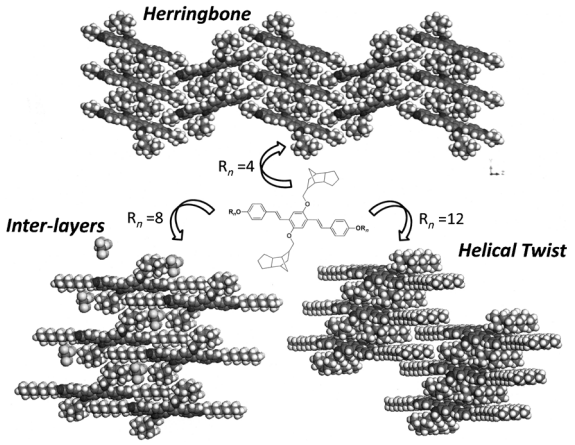


Figure 3. Three-dimensional crystal packing of OPV-4, OPV-8, and OPV-12.

π cores along the direction perpendicular to the molecular axis. The packing of these three compounds differs widely depending on the number of carbon atoms in the alkyl tails. The rigid planar aromatic core and the absence of long lateral side chains led OPV-4 to arrange in herringbone-type packing. The herringbone arrangement is one of the most stable packings for molecules in the solid state when adjacent stacks of molecules are arranged in opposite directions in the unit cell.[9] The molecular planes in the adjacent stacks are inclined with respect to each other, and the inclination is known as the herring bone (HB) angle $\xi$,[12] which is measured between molecules in adjacent stacks that are diagonally oriented to each other. The HB angle $\xi$ for OPV-4 of 81.40° (see Supporting Information SF4) is very close to perfect alignment of perpendicular herringbone sheets ($\xi =$ 90°). In herringbone-type packing so far observed for π-conjugated molecules, the absence of substituents in the central aromatic core was considered to be an important structural parameter for the existence of these patterns. Interestingly, OPV-4 is the first example of a π-conjugated system which contradicts the above assumption, since a herringbone pattern was observed despite its having large bulky TCD substituents at the central aromatic core. Increasing tail length facilitates interdigitation of tails along the molecular axis, and as a result, the molecules in OPV-8 are closely packed as bundles. The long dodecyloxy tails in OPV-12 resulted in higher-ordered structures in which the molecules are packed as columns along the *b* axis and pushed apart in the *c* axis direction. The large difference in packing of OPVs revealed that the custom designed OPV-TCD skeletons are unique in producing diverse self-assembled structures in the solid state.

The packing of the planar organic molecules in the solid state could be described in terms of two different angles, termed pitch and roll inclinations, as reported by Curtis et al.[9] A schematic diagram of pitch and roll displacements

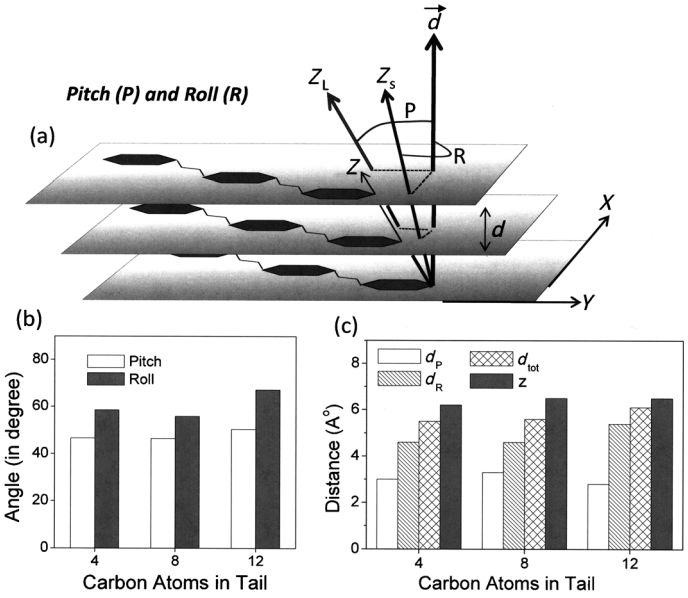


Figure 4. a) Pitch and roll displacements of OPVs and their angles (b) and distances (c) versus number of carbon atoms in the tail.

is shown in Figure 4. The planar aromatic core constitutes the *xy* molecular plane. The *x* and *y* axes are perpendicular to each other and represent the short and long axes of the molecule, respectively (see Figure 4a). The shortest distance between two adjacent molecules is defined by a vector **d** and their stacking direction along the molecular packing as a vector **z**. The pitch angle *P* and its distance $d_P$ correspond to the molecular slip along the $z_L$ direction and the vector **d**. The roll angle *R* and its distance $d_R$ are represented between the projection of molecules on the short molecular axis $Z_s$ and the **d** vector. The total slip distance $d_{tot} = \left(d_p^2 + d_r^2\right)^{1/2}$ and the crystallographic repeat distance $\mathbf{z} = \left(d_p^2 + d_r^2 + d^2\right)^{1/2}$ were obtained from the pitch and roll parameters.[9] The determination of $d_P$, $d_R$, *P*, *R*, $d_{tot}$, and **z** are given in the Supporting Information (SF-5 to SF-8). The plot of the pitch and roll angles versus the number of carbon atoms in OPV molecules (see Figure 4b) revealed that the molecules underwent a pitch-angle distortion from 46.6 to 50.4° with increasing number of C atoms in the tail. On the other hand, the roll-angle distortion was found to be much stronger, and *R* varied from 55.8 to 67.2° (≈12°). In Figure 4c, the shift distances are plotted against the number of C atoms in the tail. Among the three molecules, the pitch distance $d_P$ varied only by 0.56 Å, but the variation in the roll distance $d_R$ of 0.90 Å was almost twice the difference in pitch distances. This suggested that the effect of roll inclination in the OPV molecules is much stronger than that of displacement in the pitch direction. The increase in tail length

increases the roll angle; as a result, the OPV-12 molecules inclined more towards the *x* axis to attain layerlike self-assembly. This suggests that OPV-12 molecules have a greater tendency to pack the chromophores in parallel layers. This is further evident from the OPV-12 molecular arrangements in the crystal lattices (see Figure 3), in which each stack of molecules appears as isolated pillars along the *z* axis (direction towards **d** vector in Figure 4a). In Figure 4c, the total slip distance $d_{tot}$ and crystallographic repeat distance **z** increase with increasing number of carbon atoms in the tail. The values of $d_{tot}$ and **z** in all cases were found to be more than 5.50 Å, which is much greater than the typical aromatic π-stacking distances observed in graphite (<3.50 Å).[19] Thus, it can be concluded that these OPV molecules do not have any aromatic π-stacking interaction in the solid state. Therefore, the diversity in the self-assembly of OPV chromophores in the solid state is driven by secondary forces other than aromatic π-stacking interactions.

To trace the intermolecular interactions responsible for self-assembly in the OPVs, the close contacts between adjacent molecules were established. The close-contact interactions in the **OPV-12** molecule are shown in Figure 5. Each

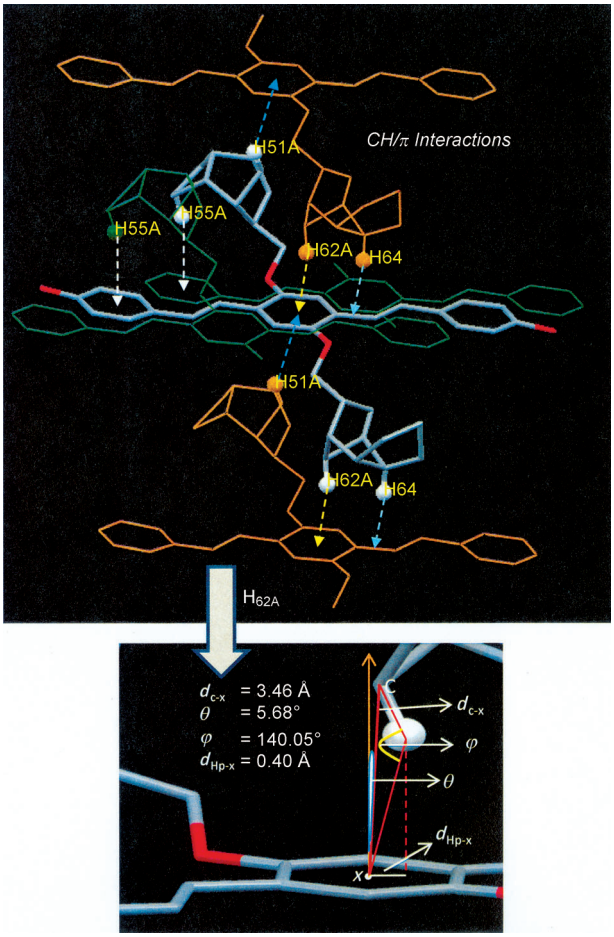


Figure 5. CH/π interactions in OPV-12 in the three-dimensional crystal lattice. In the orange and green molecules part of one of the TCD groups was omitted for clarity.

**OPV-12** molecule has close contact with four neighboring molecules. Two of the molecules (green) lie on the same plane along the *a* axis at a distance of 6.51 Å, and other two (orange) above and below the plane of the central molecule along the *b* axis at 13.23 Å. A total of eight CH/π interactions per molecule (2×4 different types) was observed between the alkyl CH groups of TCD units and the aryl rings or vinylene C=C bonds. These interactions involve $CH_{55A}$ and a terminal aryl ring, $CH_{62A}$ or $CH_{51A}$ and the central aryl ring (above and below), and $CH_{64A}$ and the vinyl C=C bond. These multiple CH/π interactions extend along the *b* axis throughout the crystal lattice. Four important crystallographic parameters describe the CH/π interactions: $d_{C-X}$, $\theta$, $\phi$, and $d_{Hp-X}$, where $d_{C-X}$ is the distance between the donor carbon atom and the center of the acceptor π ring, $\theta$ the angle between the ring normal and a vector connecting the donor carbon atom to the center of the aryl ring, $\phi$ the angle between the CH group and the vector connecting the H atom to the ring center, and $d_{Hp-X}$ the projection of the H atom on the π ring.[13a]

Determination of these CH/π crystallographic parameters is explained in the Supporting Information (SF-9). The CH/π parameters (Table 1) are in accordance with literature reports[13a] and confirm the existence of multiple-arm strong

Table 1. CH/π parameters for OPV-12.

| CH | π | $d_{C-X}$ [Å] | $\theta$ [°] | $\varphi$ [°] | $d_{Hp-X}$ [Å] |
|---|---|---|---|---|---|
| $CH_{55A}$ | aryl | 3.73 | 13.89 | 161.99 | 0.65 |
| $CH_{51A}$ | aryl | 3.61 | 10.63 | 138.16 | 1.01 |
| $CH_{62A}$ | aryl | 3.46 | 5.68 | 140.05 | 0.40 |
| $CH_{64A}$ | $C_{20}$=$C_{21}$ | 3.64 | 8.50 | 160.04 | 0.37 |

CH/π interaction in the OPV-12 molecules. The close contacts in OPV-8 were also determined as described for OPV-12 (see Supporting Information, SF-10). OPV-8 shows two identical CH/π interactions per molecule between $CH_{40A}$ and the C=C bond. However, OPV-4 did not show any CH/π interactions exhibiting the required crystallographic geometric parameters. The CH/π interactions observed in OPV-8 are completely different from those of OPV-12: 1) the H acceptor (i.e., vinyl C=C bond) in OPV-8 is relatively weak[16g] compared to the strong aryl-ring acceptor in OPV-12 and 2) the existence of multiple-arm CH/π interaction locks the 3D movement of the central aromatic core in OPV-12, which is completely absent in OPV-8. Thus, the strong multiple-arm CH/π interactions are essential for producing the hierarchical structures seen in OPV-12. Though OPV-8 has CH/π interactions, it does not show strong intermolecular locking (as seen in OPV-12) and turns out to be simple liquid-crystalline material. In the absence of CH/π interactions, OPV-4 packed in the herringbone motif. Surprisingly, the long alkyl chains did not show any type of interactions among themselves or with the aryl (or TCD) units, and therefore it can be assumed that van der Waals forces of attraction among the alkyl units are weak or

absent in the OPV molecules. Hence, it could be concluded that the multiple-arm CH/π hydrogen-bonding interactions are the prominent stabilizing force in OPVs that form higher ordered structures in the solid state (OPV-12).

The mesophase morphology of the samples in single-crystals and powder form was analyzed under a polarizing light microscope (PLM) equipped with a hot stage (see Supporting Information, SF-11 to SF-14). Single crystals of OPV-4 and OPV-8 exhibited patterns of crystalline and cholesteric mesophase, respectively (see Supporting Information, SF-11). OPV-12 showed a birefringence pattern consisting of

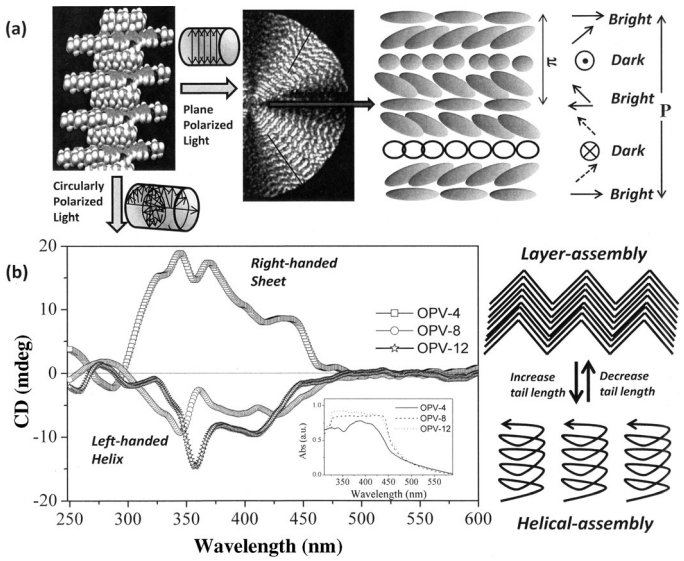


Figure 6. a) Formation of helical assemblies in OPV-12 and b) solid-state CD spectra of aligned OPV samples in the LC state (absorption spectra are shown as inset). A schematic of chain length driven self-assembly is shown bottom right.

concentric dark and bright rings (Figure 6). The mesophase morphology was identical irrespective of the sample source (single crystals or powder samples; Supporting Information, SF-11). The existence of CH/π interactions in the LC mesophase morphology, similar to the single-crystal structures, was confirmed by variable-temperature powder X-ray diffraction studies (Supporting Information, SF-15). The concentric dark and bright rings in OPV-12 are simply the Grandjean lines that are typically observed in chiral nematic N* liquid-crystalline mesophase.[20] The appearance of dark and bright lines under plane-polarized light is schematically illustrated in Figure 6a.[20] The dark lines are observed when the helical twist changes by π. From the distance $l$ between the two lines, the pitch length $p$ of the helix could be calculated as $l=p/2$. The pitch length is typically constituted by hundreds and thousands of molecules in lamellae which subsequently twist to give helical superstructure.[20] The pitch length can vary from as small as 100 nm to many micrometers. The pitch length in OPV-12 was determined to be $44.7\pm2.9$ μm. Formation of the helical assembly was not affected by cooling from the isotropic state under either non-isothermal (Supporting Information, SF-13) or isothermal (Supporting Information, SF-14) conditions. Further, the role of the number of carbon atoms in the tail in the formation of helical assemblies was also tested for OPVs with $n=$ 10–16 (Supporting Information, SF-12). The pitch lengths of helical rings gradually increased with increasing number of carbon atoms in the tail up to $n=15$ and lost this tendency at $n=16$ in OPV-16 (Supporting Information, SF-16 and SF-17). Hence, the ring-banded self-assemblies in the TCD-OPVs are a molecular property which is driven by both the number of carbon atoms in the alkyl chain and CH/π interactions.

Circular dichroism (CD) spectra of the OPVs were recorded to gain more insight into their LC mesophase helical morphology. CD spectra of OPV samples were recorded in both solution (in toluene and other solvents) as well as in the solid state (fine powder and also in aligned films). All three OPVs showed no CD signal in solution, which confirmed that they have no helical self-organization in the solution state (Supporting Information, SF-18). Therefore, the presence of a weak chiral center in the TCD units (at the bridging carbon atom $ArOCH_2C^*H$) did not provide any additional advantages for molecular self-assembly in solution. In the powder state, the samples showed very weak CD signals (Supporting Information, SF-18 and SF-19). On aligning the molecules in the thin layer (OPV-4) or LC mesophase (OPV-8 and OV-12; samples were made as per the method described for PLM studies), self-organization became predominant and strong CD signals emerged from the samples. Hence, alignment of the organic molecules promoted self-organization of OPVs in the solid state. The CD spectra and absorption spectra of OPVs are shown in Figure 6b. All three OPVs showed broad absorption spectra from 300 to 500 nm and their CD spectra were observed in the same region as their absorption spectra. OPV-4 showed a strong positive Cotton effect with maximum at 345 nm and zero crossing at 295 nm. This indicated that the OPV-4 molecules are arranged as right-handed sheetlike structures (as seen in the herringbone layers in Figure 2). In contrast, OPV-8 and OPV-12 showed intense negative CD signals corresponding to absorption of left circularly polarized light (negative Cotton effect). The CD spectrum of OPV-12 showed two strong negative bands at 357 and 408 nm and a weak positive band at 275 nm (OPV-8 also showed a similar trend). The features of these negative signals in OPV-12 (and also in OPV-8 and OPV-11) confirmed that the molecules were arranged in the left-handed helical assembly. Hence, the helical lines observed under the plane-polarized illumination in OPV-12 molecules (see Figure 6a) are nothing but helical self-assemblies of the lamella in the solid state. Thus, for the first time, a perfect correlation between the LC helical mesophase (observed under PLM) with the helical supramolecular structures (in CD signals) was established in solid-state self-assembly.

The photophysical characterization of OPV chromophores showed that the emission spectra of OPV-4, OPV-8, and

OPV-12 in both LC phase and single crystals are almost identical, with maxima at 490 nm. Furthermore, time-dependent fluorescence time decay measurements by the time-correlated single-photon counting technique (details are provided in Supporting Information, SF-20) revealed that the OPV chromophores show almost identical lifetimes irrespective of their occupancy either in herringbone sheets (OPV-4) or in helical self-assembly (OPV-12 and OPV-8). The absence of aromatic π-stacking interactions (responsible for photophysical variation) among the chromophores accounts for this similarity in PL characteristics. In our previous work, we noticed that the π-stacking interaction was completely absent in undecyl-substituted OPV, which is completely different from the TCD-OPVs.[17] Currently, we are studying the role of π-stacking in the OPVs having substituents other than TCD (e.g., branched ethylhexyl or linear octyl chains). A preliminary crystal structure analysis (see Supporting Information, SF-21) revealed that the π-stacking interaction is also not present in other OPV molecules. Therefore, the lack of π-stacking interaction found in the present investigation is not restricted to TCD-OPVs, and it is also generally applicable to other OPVs. Thus, without altering luminescent characteristics of the π-conjugated chromophores, diverse self-assembly was achieved by only varying the number of carbon atoms in the tails (see Figure 6). Increasing the number of carbon atoms in the tail transformed the chromophore packing from herringbone to left-handed helical twist in the chiral nematic mesophase. On the other hand, on decreasing the tail length, the chromophores organized in highly packed herringbone patterns. For longer alkyl chains ($n \geq 14$), the packing of the chromophores is no longer controlled by the tails and the molecular self-assemblies are lost. The CH/π interactions were found to be a crucial stabilizing factor in aligning the chromophores in the long-tailed OPVs (OPV-10 to OPV-15); a result, the chromophores transformed into helical supramolecular assemblies.

## Conclusion

Direct evidence for the CH/π interaction was established on the basis of crystal structures of OPVs. The existence of multiple-arm CH/π interaction was identified as the main driving force for helical self-assembly in the liquid-crystalline phase. Planar OPV chromophores (π acceptor) were designed with suitable bulky TCD units as C–H bond donor and carbon-atom tails as self-assembly director to demonstrate the importance of CH/π interactions in supramolecular chemistry. The large pitch and roll displacements completely destroy the aromatic π-stacking interactions among the OPV chromophores. The larger roll displacements (67.2°) caused the OPV-12 molecules to incline towards the crystallographic *b* axis. The existence of multiple CH/π interactions in OPV-12 stabilizes these molecules; as a result, OPV-12 exhibits helical self-assembly in the thermotropic LC mesophase. The existence of left-handed helicity in OPV-12 was further proved by a CD investigation in the solid state. OPV-4 adopts a herringbone layer pattern and forms right-handed sheetlike structures. The uniqueness of the present approach is that both herringbone and helical assemblies could be simply varied by means of the number of carbon atoms in the tails. Though the approach demonstrated here describes in detail the role of CH/π interactions in OPVs, it is not restricted to any particular type of π-conjugated oligomers. The overall findings revealed that the CH/π interaction is a very powerful noncovalent interaction in supramolecular chemistry. This finding is just the tip of the iceberg in the ocean of molecular self-organization and has great potential for breakthrough discoveries in π-conjugated materials.

## Experimental Section

Syntheses and characterization of compounds, crystallographic images, unit cells, calculation of pitch and roll parameters, CH/π interaction parameters, DSC traces, temperature-dependent PLM textures, WXRD plots, emission spectra and TCSPC life time plots and data, CD signals for solution and powder samples, and $^{1}$H NMR, $^{13}$C NMR, MALDI mass spectra are provided in the Supporting Information. CCDC 846783, 846784 and 846785 contain the supplementary crystallographic data for this paper. These data can be obtained free of charge from The Cambridge Crystallographic Data Centre via www.ccdc.cam.ac.uk/data_request/cif.

## Acknowledgements

Research grant from Department of Science and Technology (DST), New Delhi, India under nanomission initiative project SR/NM/NS-42/2009 is acknowledged. M.G. thanks CSIR, India for SRF fellowship.

[1] H. Sirringhaus, P. J. Brown, R. H. Friend, M. M. Nielsen, K. Bechgaard, B. M. W. Langeveld-Voss, A. J. H. Spiering, R. A. J. Janssen, E. W. Meijer, P. Herwig, D. M. de Leeuw, *Nature* **1999**, *401*, 685-688.
[2] A. N. Sokolov, A. A. Evrenk, R. Mondal, H. B. Akkerman, R. S. S. Carrera, S. G. Focil, J. Schrier, S. C. B. Mannsfeld, A. P. Zoombelt, Z. Bao, A. A. Guzik, *Nat. Commun.* **2011**, *2:437*, 1–8.
[3] K. Muller, G. Wegner, *Electronic Materials: The Oligomer Approach*, Wiley-VCH, Weinheim, **1998**.
[4] R. Österbacka, C. P. An, X. M. Jiang, Z. V. Vardeny, *Science* **2000**, *287*, 839–842.
[5] a) A. P. H. J. Schenning, P. Jonkheijm, E. Peeters, E. W. Meijer, *J. Am. Chem. Soc.* **2001**, *123*, 409–416; b) S. K. Asha, A. P. H. J. Schenning, E. W. Meijer, *Chem. Eur. J.* **2002**, *8*, 3353–3361; c) J. V. van Herrikhuyzen, S. K. Asha, A. P. H. J. Schenning, E. W. Meijer, *J. Am. Chem. Soc.* **2004**, *126*, 10021–10027; d) A. Ajayaghosh, C. Vijayakumara, R. Varghese, S. J. George, *Angew. Chem.* **2006**, *118*, 470–474; *Angew. Chem. Int. Ed.* **2006**, *45*, 456–460; e) S. S. Babu, V. K. Praveen, S. Prasanthkumar, A. Ajayaghosh, *Chem. Eur. J.* **2008**, *14*, 9577–9584; f) Y. Hirai, S. S. Babu, V. K. Praveen, T. Yasuda, A. Ajayaghosh, T. Kato, *Adv. Mater.* **2009**, *21*, 4029–4033.
[6] a) J. B. Beck, S. J. Rowan, *J. Am. Chem. Soc.* **2003**, *125*, 13922–13923; b) S. Ghosh, S. Ramakrishnan, *Angew. Chem.* **2005**, *117*, 5577–5583; *Angew. Chem. Int. Ed.* **2005**, *44*, 5441–5447; c) S. Ghosh, S. Ramakrishnan, *Angew. Chem.* **2004**, *116*, 3326–3330; *Angew. Chem. Int. Ed.* **2004**, *43*, 3264–3268.

  

[7] a) R. S. Lokey, B. L. Iverson, *Nature* **1995**, *375*, 303–305; b) P. Osswald, D. Leusser, D. Stalke and F. Würthner, *Angew. Chem.* **2005**, *117*, 254–257; *Angew. Chem. Int. Ed.* **2005**, *44*, 250–253; c) G. A. Bhavsar, S. K. Asha, *Chem. Eur. J.* **2011**, *18*, 12646–12658; d) M. Prehm, F. Liu, X. Zeng, G. Ungar, C. Tschierske, *J. Am. Chem. Soc.* **2011**, *133*, 4906–4916.

[8] a) D. Holmes, S. Kumarasamy, A. J. Matzger, K. P. C. Vollhardt, *Chem. Eur. J.* **1999**, *5*, 3399–3412; b) G. Horowitz, B. Bachet, A. Yassar, P. Lang, F. Damanze, J. L. Fave, F. Garnier, *Chem. Mater.* **1995**, *7*, 1337–1341.

[9] M. D. Curtis, J. Cao, J. W. Kampf, *J. Am. Chem. Soc.* **2004**, *126*, 4318–4328.

[10] a) J. Gierschner, M. Ehni, H. J. Egelhaaf, B. M. Medina, D. Beljonne, *J. Chem. Phys.* **2005**, *123*, 144914–144914; b) C. Zhao, Z. Wang, Y. Yang, C. Feng, W. Li, Y. Li, Y. Zhang, F. Bao, Y. Xing, X. Zhang, X. Zhang, *Cryst. Growth Des.* **2012**, *12*, 1227–1231; c) S. J. Yoon, S. Y. Park, *J. Mater. Chem.* **2011**, *21*, 8338–8346; d) R. E. Gill, P. F. V. Hutten, A. Meetsma, G. Hadziioannou, *Chem. Mater.* **1996**, *8*, 1341–1346; e) R. E. Gill, A. Meetsma, G. Hadziioannou, *Adv. Mater.* **1996**, *8*, 212–214; f) Z. Xie, H. Wang, F. Li, W. Xie, L. Liu, B. Yang, L. Ye, Y. Ma, *Cryst. Growth Des.* **2007**, *7*, 2512–2516; g) C. Melzer, M. Brinkmann, V. V. Krasnikov, G. Hadziioannou, *ChemPhysChem* **2005**, 6, 2376–2382.

[11] C. Wang, H. Dong, H. Li, H. Zhao, Q. Meng, W. Hu, *Cryst. Growth Des.* **2010**, *10*, 4155–4160.

[12] S. Varghese, S. Das, *J. Phys. Chem. Lett.* **2011**, *2*, 863–873 and references are cited therein.

[13] a) M. Brandl, M. S. Weiss, A. Jabs, J. Suhnel, R. Hilgenfeld, *J. Mol. Biol.* **2001**, *307*, 357–377; b) P. Chakrabarti, U. Samanta, *J. Mol. Biol.* **1995**, *251*, 9–14; c) M. Nishio, M. Hirota, Y. Umezawa, *The CH-π interaction. Evidence, Nature and Consequences*, Wiley-VCH, Weinheim, **1998**.

[14] a) B. Bhayana, C. S. A. Wilcox, *Angew. Chem. Int. Ed.* **2007**, *46*, 6833–6836; b) C. A. Sacksteder, S. L. Bender, B. A. Barry, *J. Am. Chem. Soc.* **2005**, *127*, 7879–7890.

[15] a) G. R. Desiraju, *Acc. Chem. Res.* **2002**, *35*, 565–573; b) T. Steiner, G. R. Desiraju, *Chem. Commun.* **1998**, 891–892; c) G. R Desiraju, T. Steiner, *The weak Hydrogen Bond*, Oxford University Press, London, **1999**.

[16] a) E. Kim, S. Paliwal, C. S. Wilcox, *J. Am. Chem. Soc.* **1998**, *120*, 11192–11193; b) K. Dziubek, M. Podasiadlo, A. Katrusiak, *J. Am. Chem. Soc.* **2007**, *129*, 12620–12621; c) L. S. Birchall, S. Roy, V. Jayawarna, M. Hughes, E. Irvine, G. T. Okorogheye, N. Saudi, E. D. Santis, T. Tuttle, A. A. Edwards, R. V. Ulijn, *Chem. Sci.* **2011**, *2*, 1349–1355; d) M. Yamakawa, I. Yamada, R. Noyori, *Angew. Chem.* **2001**, *113*, 2900; *Angew. Chem. Int. Ed.* **2001**, *40*, 2818- 2821; e) B. W. Gung, B. U. Emenike, M. Lewis, K. Kirschbaum, *Chem. Eur. J.* **2010**, *16*, 12357–12362; f) K. Kobayashi, K. Ishii, S. Sakamoto, T. Shirasaka, K. Yamaguchi, *J. Am. Chem. Soc.* **2003**, *125*, 10615–10624; g) P. Tarakeshwar, H. S. Choi, K. S. Kim, *J. Am. Chem. Soc.* **2001**, *123*, 3323–3331.

[17] M. Goel, M. Jayakannan, *Chem. Eur. J.* **2012**, *18*, 2867–2874.

[18] a) M. Goel, M. Jayakannan, *J. Phys. Chem. B* **2010**, *114*, 12508–12519; b) S. R. Amrutha, M. Jayakannan, *J. Phys. Chem. B* **2009**, *113*, 5083–5091.

[19] C. H. Desch. *The Chemistry of Solids*, Cornell University Press, Ithaca, **1934**, pp. 180–181.

[20] I. Dierking, *Textures of Liquid Crystals*, 2nd ed.; Wiley-VCH, Weinheim, **2003**.

Received: March 2, 2012
Revised: June 11, 2012
Published online: ■■ ▮▮, 0000

  

Supramolecular Chemistry

*M. Goel, M. Jayakannan* . .* ■■■■–■■■■

**Herringbone and Helical Self-Assembly of π-Conjugated Molecules in the Solid State through CH/π Hydrogen Bonds**

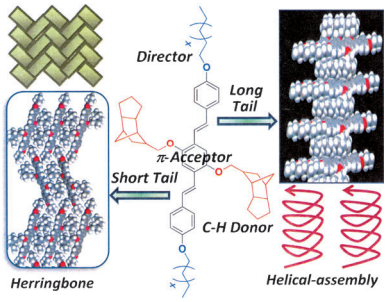


**Multiple CH/π interactions** drive self-organization of custom-designed oligophenylenevinylenes with a distyrylbenzene core as π acceptor, bulky tricyclodecanemethylene groups as CH donors, and alkyl tails as self-assembly directors. Both herringbone and helical supramolecular structures could be obtained in the solid state simply by varying the number of carbon atoms in the tails (see figure).■■original text was too long, ok?■■